ELSEVIER

Journal of Alloys and Compounds 293–295 (1999) 178–184

Journal of ALLOYS AND COMPOUNDS

Crystal and magnetic structure of TbNiAl-based deuterides, $TbNiAlD_{0.30}$ and $TbNiAlD_{1.04}$, studied by neutron diffraction and synchrotron radiation

B.C. Hauback[a,*], H. Fjellvåg[a,c], L. Pålhaugen[a], V.A. Yartys[a,b], K Yvon[d]

[a]*Institute for Energy Technology, P.O. Box 40, N-2027 Kjeller, Norway*

[b]*Metal Hydrides Department, Karpenko Physico-Mechanical Institute of the National Academy of Sciences of Ukraine, 5, Naukova Str., Lviv 290601, Ukraine*

[c]*Department of Chemistry, University of Oslo, N-0315 Oslo, Norway*

[d]*Laboratoire de Cristallographie, Université de Genève, 24 quai Ernest Ansermet, CH-1211 Genève 4, Switzerland*

Abstract

The crystal structure of the two lower deuterides $TbNiAlD_{0.30}$ and $TbNiAlD_{1.04}$ formed by intermetallic TbNiAl have been studied by neutron and synchrotron X-ray powder diffraction at room temperature. In addition, neutron diffraction at low temperature has been used to study the magnetic properties of $TbNiAlD_{0.30}$. Both deuterides were prepared by deuterium desorption from the saturated deuteride $TbNiAlD_{1.4}$. For $TbNiAlD_{0.30}$, superstructure reflections in the room temperature neutron pattern suggest space group *P62c* and a doubling of the *c*-axis [$a=7.0433(1)$, $c=7.7826(1)$ Å] relative to the intermetallic compound. Deuterium occupies every second trigonal bipyramidal Tb_3Ni_2 interstice along *c* (91% occupancy), and the compound orders antiferromagnetically below $T_N=42$ K. Its magnetic structure at 7 and 28 K has two terbium sublattices, both with the same propagation vector $\mathbf{k}=(1/2, 1/2, 1)$, but with significantly different magnetic moments of 8.0(1) and 1.3(1) μ_B per Tb atom (at 7 K). The structure of $TbNiAlD_{1.04}$ is described in space group *Amm2* [$a=3.8257(1)$, $b=12.4668(5)$, $c=7.2964(3)$ Å; orthorhombic distortion $b/c=0.986\sqrt{3}$]. Three different sites are occupied by deuterium, corresponding to one trigonal bipyramidal Tb_3Ni_2 type (88% occupancy) and two tetrahedral Tb_2NiAl-type interstices (50 and 18% occupancy).

Keywords: Deuterides; Rare-earth intermetallic compound; Neutron diffraction; Synchrotron radiation; Crystal and magnetic structure

1. Introduction

The intermetallic compound TbNiAl crystallises with the ZrNiAl type structure (hexagonal, space group *P62m*). It absorbs up to 1.4 hydrogen (deuterium) atoms per formula unit at room temperature and 1 bar H_2/D_2 pressure. Hydrogenation (deuteration) leads to an orthorhombic distortion. Three interstitial positions are occupied by deuterium atoms in the orthorhombic $TbNiAlD_{1.1}$ deuteride [space group *Amm2*, $a=3.7209(7)$, $b=12.4011(3)$, $c=7.6075(2)$ Å], one Tb_3Ni_2 trigonal bipyramidal position (D1; 88% occupancy) and two interstices with tetrahedral Tb_2NiAl surroundings (67 and 10% occupation in D2 and D3, respectively) [1]. Deuterium desorption from the saturated deuteride proceeds in a wide temperature range from 298 to about 800 K with distinct peaks at 463 and 723 K. Other known crystal structures of ZrNiAl-type deuterides determined by neutron diffraction are $ZrNiAlD_{0.57}$ [2], $Zr_6FeAl_2D_{10}$ [3] and $TbNiAlD_{1.28}$ [4].

The present neutron and synchrotron X-ray study focuses on the room temperature structure of two lower deuterides of TbNiAl, having the compositions $TbNiAlD_{0.30}$ and $TbNiAlD_{1.04}$. The change of magnetic properties upon deuteration and the structures at low temperatures will be discussed in more detail elsewhere [5].

2. Experimental details

The TbNiAl intermetallic compound was prepared by argon arc melting of a mixture of high purity terbium (99.8%), nickel (99.9%) and aluminium (99.9%). Details of the preparation of TbNiAl are given in [1]. The unit-cell dimensions, $a=6.999(1)$ and $c=3.879(2)$ Å, as determined from powder X-ray diffraction (PXD, Siemens D5000 diffractometer, Bragg-Brentano geometry, $CuK\alpha_1$-radia-

*Corresponding author. Tel.: +47-638-06078; fax: +47-638-10920.
E-mail address: bjorn@ife.no (B.C. Hauback)

0925-8388/99/$ – see front matter
PII: S0925-8388(99)00417-X

tion, position sensitive detector), agreed well with literature data [6].

The deuterated samples were prepared by a step-by-step desorption procedure. Prior to deuteration, the samples were activated by heating under secondary vacuum at 673 K for 1 h. Saturated $TbNiAlD_{1.4}$ deuteride was synthesised at room temperature and at a deuterium (99.8% purity) pressure below 1 bar. Two lower deuterides, $TbNiAlD_{0.3}$ and $TbNiAlD_{1.0}$, were synthesised from $TbNiAlD_{1.4}$ by applying a secondary vacuum at 490 and 298 K, respectively. Nearly single-phase deuterides, with a small additional contribution from unidentified phases, were confirmed from PXD data.

Powder neutron diffraction (PND) data were collected with the PUS instrument accommodated at the JEEP II reactor at Kjeller. Monochromatized neutrons were obtained by reflection from Ge(511) of the focusing composite germanium monochromator with an approximately 90° take-off angle. The detectors consist of two banks of seven position sensitive ^{3}He detectors, each covering 20° in 2θ. A cylindrical sample holder of vanadium with 5-mm inner diameter was used. Temperatures between 7 and 300 K were obtained by a Displex cooling system.

Synchrotron (SR) PXD data were collected with the powder diffractomter (in Debye-Scherrer mode) at the Swiss Norwegian Beam Line (BM1) at ESRF (Grenoble). Monochromatic X-rays were obtained from a channel-cut Si(111) crystal. The samples were contained in a rotating 0.3-mm diameter sealed glass capillary.

The GSAS program package [7] was used for the combined Rietveld-type profile refinements of the powder synchrotron X-ray and neutron diffraction data collected at 298 K. Table 1 summarizes characteristics of the data sets. The initial structural model for both $TbNiAlD_{0.3}$ and $TbNiAlD_{1.0}$ were based on the description of $TbNiAlD_{1.1}$ [1]. Soft constraints on the Ni–D and Al–D distances were used in the refinements for $TbNiAlD_{1.0}$.

The scattering lengths $b_{Tb}=7.38$, $b_{Ni}=10.30$, $b_{Al}=3.45$ and $b_D=6.67$ fm and X-ray form-factor coefficients were taken from the GSAS library. The peak profiles of the synchrotron diffraction patterns were modelled by a pseudo-Voight function, for the PND data a Gaussian function was used. Cosine Fourier series polynomials were used to model the background of all data sets. The FULLPROF program [8] was used for Rietveld refinements of PND data collected at 7 and 28 K for $TbNiAlD_{0.3}$ (crystal and magnetic structure).

Table 1
Summary of experimental details

	$TbNiAlD_{0.30}$		$TbNiAlD_{1.04}$	
	PND	PXD(SR)	PND	PXD(SR)
Wavelength (Å)	1.5470	0.65015	1.5565	0.65015
2θ-range (°)	10–130	5.50–37.85	10–130	5.50–40.00
$\Delta 2\theta$ (°)	0.05	0.005	0.05	0.010
No. of data points	2400	6471	2400	3450
No. of reflections	135	89	198	152
No. of variables[a]	44	44	89	89

[a] Total number of variables for the combined PND and PXD(SR) refinements.

3. Results and discussion

3.1. Room temperature structure of $TbNiAlD_{0.30}$

The laboratory PXD pattern for $TbNiAlD_{0.30}$ was indexed on the same hexagonal unit cell as for the TbNiAl intermetallic compound. The volume expansion was 1.6% ($\Delta a/a=0.63\%$, $\Delta c/c=0.32\%$). Synchrotron PXD was carried out in order to find indications of an orthorhombic distortion as observed for the higher deuterides, but no significant diffraction line splittings were observed. Initial refinements on the PND data in the space group $P\bar{6}2m$ (No. 189) showed that Tb_3Ni_2 bipyramids (2*d* sites) are the only type of interstices occupied by deuterium. However, the presence of additional reflections, of which the strongest ones are marked in Fig. 1(a), required a doubling of the hexagonal *c*-axis. A few such reflections were also observed in the PXD(SR) pattern, and could be indexed on the same superstructure cell. Both PXD(SR) and PND data could be refined in space group $P\bar{6}2c$ (No. 190). Unit cell dimensions (from the synchrotron data) and agreement factors of a Rietveld-type profile refinement of the combined PND and PXD(SR) data are given in Table 2, and refined atomic parameters in Table 3. The observed, calculated and difference PND and PXD(SR) profiles are shown in Fig. 1. The results indicate that deuterium desorption of $TbNiAlD_{1.4}$ does not proceed uniformly over the structure. As shown in Fig. 2, the D atoms in $TbNiAlD_{0.3}$ no longer occupy the tetrahedral Tb_2NiAl interstices, and fill only half of the trigonal bipyramidal Tb_3Ni_2 type interstices centred at 1/3, 2/3, 1/4 (site 2*c*) and 2/3, 1/3, 3/4 (site 2*d*). The exclusive and almost full occupancy of site 2*c* leads to an alternating deuterium occupancy along the hexagonal axis and thus the observed superstructure along *c*. As a consequence, the metal environment around the empty 2*d* sites (Tb-2*d*=2.041 Å) is significantly contracted compared to that around the occupied 2*c* sites (Tb-D=2.209(2) Å). The nickel–deuterium distances are Ni(1)–D=1.848(3) Å, while the D–D separation substantially exceeds the 2.0 Å limit. The deuterium–metal distances in $TbNiAlD_{0.30}$ are close to the corresponding distances in the Tb_3Ni_2 trigonal bipyramids in $TbNiAlD_{1.1}$ (Tb–D1=2.20–2.28 Å; Ni–D1=1.853 Å). In conclusion, the lower deuteride $TbNiAlD_{0.3}$ has a structure which is nearly ordered at room temperature and has the ideal stoichiometry $TbNiAlD_{0.333}$. Its deuterium atoms occupy half of the available trigonal bipyramidal sites [site 2*c* in space group $P\bar{6}2c$, refined occupancy 0.91(2)]. The more deuterium-rich deuteride $ZrNiAlD_{0.57}$

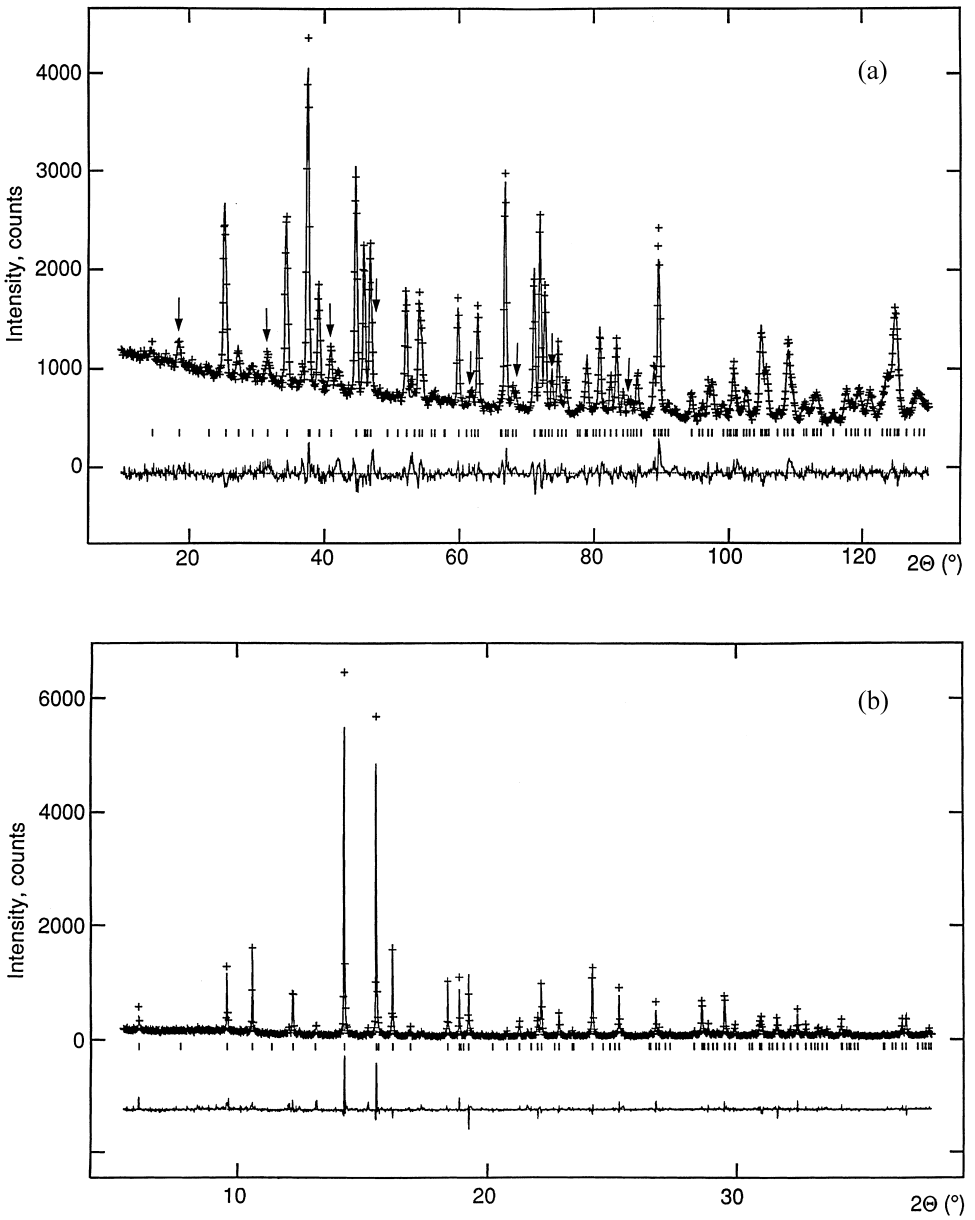

Fig. 1. (a) PND, with the strongest superstructure reflections marked with arrows; and (b) PXD(SR) patterns for $TbNiAlD_{0.30}$ at 298 K showing observed (+), calculated (line) and difference (line at bottom) plot.

Table 2
Cell parameters at 298 K and reliability factors[a]

	$TbNiAlD_{0.30}$	$TbNiAlD_{1.04}$
Space group	$P\bar{6}2c$ (No. 190)	*Amm2* (No. 38)
a (Å)	7.0433(1)	3.8257(1)
b (Å)		12.4668(5)
c (Å)	7.7826(1)	7.2964(3)
V (Å^3)	334.36(1)	347.98(3)
R_p (%) PXD(SR)	11.0	11.0
R_{wp} (%) PXD(SR)	14.3	14.4
R_p (%) PND	4.0	4.3
R_{wp} (%) PND	5.3	5.5
χ^2	2.77	3.16

[a] Calculated standard deviations in parentheses.

[2], by comparison, has a disordered structure at room temperature in which the D atoms fill all trigonal bipyramidal sites in a uniform manner [site 2*d* in $P\bar{6}2m$, refined occupancy 0.85(3)].

3.2. Room temperature structure of $TbNiAlD_{1.04}$

The structure of $TbNiAlD_{1.04}$ is described in the orthorhombic space group *Amm2* (No. 38). Refined cell parameters at room temperature (from synchrotron data) are presented in Table 2. The orthorhombic distortion from the hexagonal symmetry, given by $b/c=0.986\sqrt{3}$ ($\Delta a/c_{hex}=-1.4\%$, $\Delta c/a_{hex}=4.2\%$), is significantly smaller than for the previously investigated deuteride $TbNiAlD_{1.1}$ [1]

Table 3
Atomic coordinates and displacement parameters (in 10^{-2}Å^2) from the combined PND and PXD(SR) Rietveld analysis for $TbNiAlD_{0.30}$ at 298 K

Atom	Site	*x*	*y*	*z*	U_{iso}	Occupancy
Tb	*6h*	0.5947(2)	0.0144(3)	1/4	0.45(3)	1
Ni1	*4f*	1/3	2/3	0.0125(4)	1.00(4)	1
Ni2	*2b*	0	0	1/4	1.00(4)	1
Al	*6g*	0.2354(6)	0	0	1.40(11)	1
D	*2c*	1/3	2/3	1/4	0.99(19)	0.91(2)

which has a b/c ratio of $0.941\sqrt{3}$. Because of its similar deuterium content, its total volume expansion, $\Delta V/V$= 5.7%, is only slightly smaller than for $TbNiAlD_{1.1}$ ($\Delta V/V$ 6.1%).

Table 4 gives refined coordinates and displacement parameters from the Rietveld refinements. PND and PXD(SR) profiles are shown in Fig. 3. The structure of

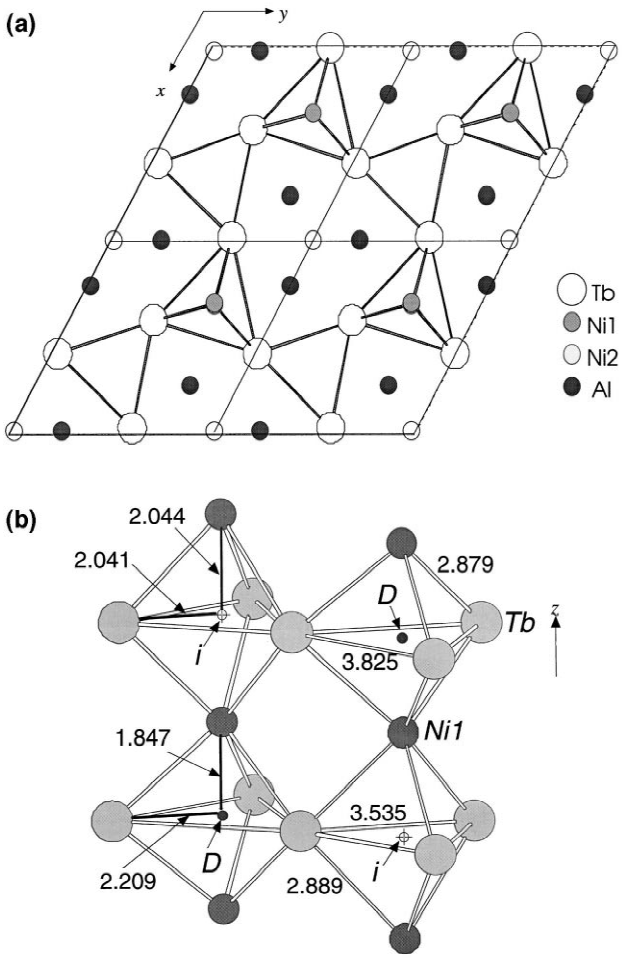

Fig. 2. (a) The alternating filled and empty Tb_3Ni1_2 interstices in the structure of hexagonal $TbNiAlD_{0.30}$ viewed along [001] for $0<z<1/2$. The D sites overlap with Ni1. (b) The two types of Tb_3Ni_2 trigonal bipyramids, filled (D) and empty (i), in $TbNiAlD_{0.30}$.

$TbNiAlD_{1.04}$ (Fig. 4) contains three partially occupied deuterium sites, one situated in a trigonal–bipyramidal Tb_3Ni_2-type interstice (D1, occupancy 0.88(2)) and two in tetrahedral Tb_2NiAl types interstices (occupancies 0.50(3) for D2 and 0.18(3) for D3). A comparison between $TbNiAlD_{1.04}$ and $TbNiAlD_{1.1}$ shows interesting differences. While D1 and D2 occupy the same interstites in both compounds, the D3 positions are located in different tetrahedral Tb_2NiAl interstices (see sites labelled D3 and D3′ in Fig. 4) and have different occupancies in $TbNiAlD_{1.04}$ (D3: 0.18) and $TbNiAlD_{1.1}$ (D3′: 0.10). As to the occupancy of D2, it is significantly lower in $TbNiAlD_{1.04}$ (D2: 0.50) compared to more deuterium rich $TbNiAlD_{1.1}$ (D2: 0.67). These features are presumably related to the rather different orthorhombic lattice distorsions of these two compounds. In particular, the more uniform deuterium distribution in $TbNiAlD_{1.04}$ (occupancy ratio D2/D3=2.8) compared to $TbNiAlD_{1.1}$ (occupancy ratio D2/D3′=6.7) correlates with the more isotropic lattice expansion of the former compound compared to that of the latter. It should be noted that the experimentally observed limit of the deuterium solubility in TbNiAl is 1.4 deuterium atoms per formula unit [9] and thus requires a three-site model in contrast to a two-site site model such as that proposed for $TbNiAlD_{1.28}$ [4] which is limited to 1.333 deuterium atoms per formula unit.

The metal–deuterium distances are Tb–D=2.18–2.41, Ni–D=1.52–1.91, Al–D=1.63–1.64 Å. Again the Tb1–D1 distances in the Tb_3Ni_2 sites in $TbNiAlD_{1.04}$, 2.19(2)–

Table 4
Atomic coordinates and displacement parameters (in 10^{-2}Å^2) from the combined PND and PXD(SR) Rietveld analysis for $TbNiAlD_{1.04}$ at 298 K

Atom	Site	*x*	*y*	*z*	U_{iso}	Occupancy
Tb1	*4e*	1/2	0.2062(2)	0.025(3)	0.36(6)	1
Tb2	*2b*	1/2	0	0.642(3)	0.36(6)	1
Ni1	*4d*	0	0.3309(5)	0.237(3)	1.57(10)	1
Ni2	*2b*	1/2	0	0.232(3)	1.57(10)	1
Al1	*4d*	0	0.123(1)	0.333(3)	1.7(3)	1
Al2	*2a*	0	0	0(−)	1.7(3)	1
D1	*4e*	1/2	0.334(1)	0.233(4)	3.3(3)	0.88(2)
D2	*4d*	0	0.394(1)	0.056(3)	3.3(3)	0.50(3)
D3	*4d*	0	0.2135(7)	0.168(3)	3.3(3)	0.18(3)

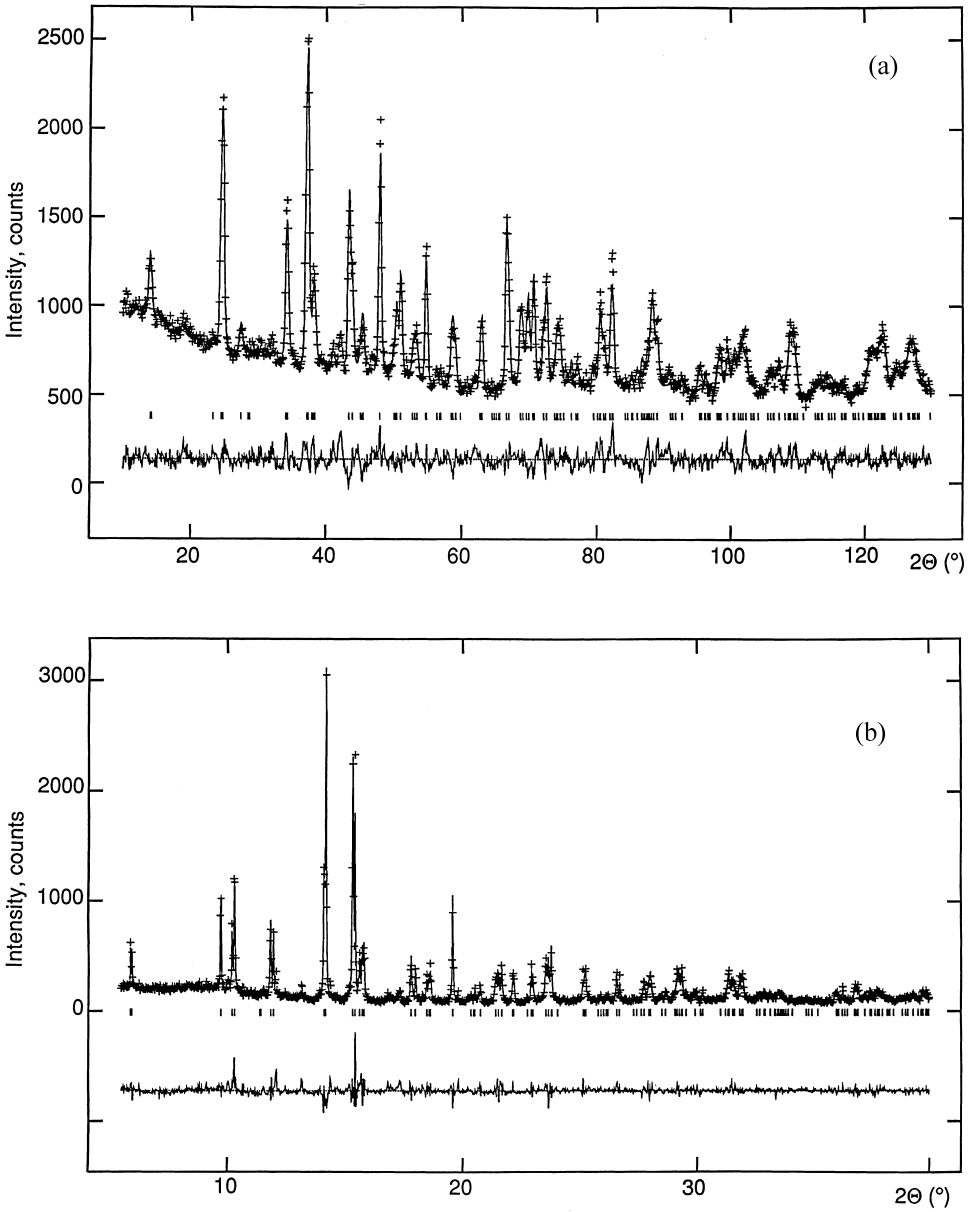

Fig. 3. (a) PND and (b) PXD(SR) patterns for $TbNiAlD_{1.04}$ at 298 K showing observed (+), calculated (line) and difference (line at bottom) plots.

2.20(2), are equal to the Tb–D distance in $TbNiAlD_{0.30}$ [2.209(2) Å]. However, Ni–D1 is noticeably longer in $TbNiAlD_{1.04}$, 1.913(1) Å, than in $TbNiAlD_{0.30}$, 1.848(3) Å. The shortest deuterium–deuterium contact distance is 2.39 Å.

3.3. Low-temperature structure and magnetic ordering of $TbNiAlD_{0.30}$

An antiferromagnetic (AF) ordering was observed below T_N=42 K for $TbNiAlD_{0.30}$ both from magnetisation measurements and neutron diffraction. The magnetic structure can be described in a hexagonal unit cell with doubled *a*-axis relative to the room temperature structure. This is the same magnetic unit cell that was used to describe the magnetic ordering in the intermetallic compound TbNiAl which has a slightly higher magnetic ordering temperature T_N=47 K [10]. The magnetic Tb atoms are ordered in two sublattices, both with the same propagation vector **k**=(1/2, 1/2, 1). The second sublattice consists of frustrated spins. The magnetic moments are parallel or anti-parallel to the crystallographic *c*-axis. This description is equal to the high-temperature AF region for TbNiAl (23–47 K) [9].

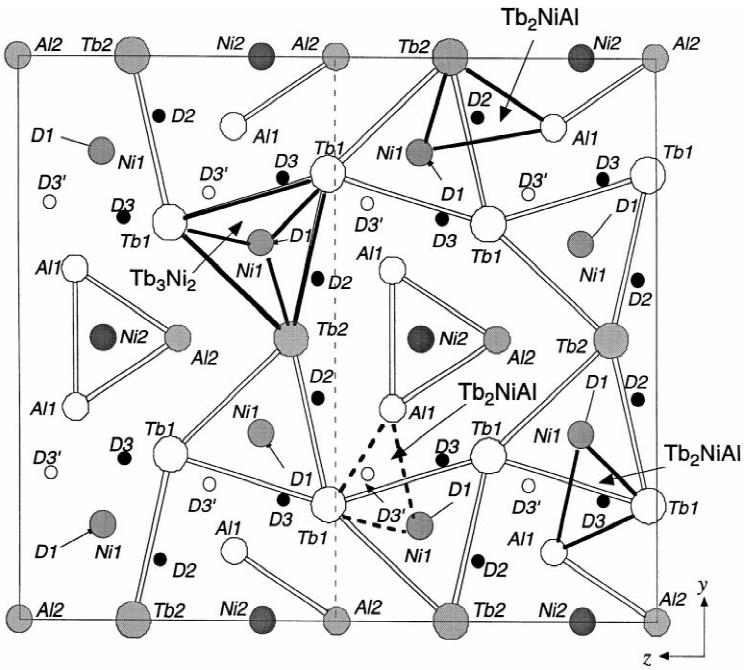

Fig. 4. Structure of orthorhombic $TbNiAlD_{1.04}$ viewed along [100] with deuterium in D1, D2 and D3. For comparison the D3′ position of $TbNiAlD_{1.1}$ (called D3 in Ref. [1]) is shown.

The magnetic moments of the two sublattices of $TbNiAlD_{0.30}$ are 8.0(1) and 1.3(1) μ_B at 7 K, and 6.9(1) and 1.4(1) μ_B at 28 K. Thus the frustrated spins in the deuteride have smaller moment values than in the alloy (2.9 μ_B at 23 K), while the moments of the other sublattice have about the same value. As to the magnetic structure previously observed for TbNiAl in the temperature region 2–23 K [9] no such structure appeared for $TbNiAlD_{0.30}$ down to 7 K. Details of the magnetisation measurements and the crystal and magnetic structures of the TbNiAl deuterides at low temperatures will be presented in a forthcoming paper [5].

4. Conclusions

Despite their relatively small range of existence, TbNiAl-based deuterides form various distinct and crystallographically different phases. Hexagonal $TbNiAlD_{0.30}$ forms a superstructure which appears to be induced by an ordering of the deuterium atoms over half of the available Tb_3Ni_2 bipyramidal interstices. This leads to a symmetry change from space group *P62m* to *P62c* and a doubling of the *c*-axis. Its antiferromagnetic structure at 7 K is similar to that found at higher temperatures for intermetallic TbNiAl. It consists of two Tb sublattices whose spins are aligned along the *c*-axis and have significantly different moment values.

In orthorhombic $TbNiAlD_{1.04}$ three types of interstitial positions are filled, one Tb_3Ni_2 trigonal bipyramid, and two Tb_2NiAl tetrahedra. The relative arrangement of the latter positions differs, however, from that in the previously studied $TbNiAlD_{1.1}$, thus leading to a substantial degree of freedom for the orthorhombic lattice distortion. This underlines the great flexibility of the metal sublattice in metal hydrides and the relatively large inventory of metal–hydrogen bonding interactions.

Acknowledgements

This work has received financial support from the Research Council of Norway and Hydro Megon. The possibility of collecting diffraction data at the Swiss-Norwegian Beam Line at ESRF, Grenoble, is gratefully acknowledged.

References

[1] V.A. Yartys, F. Gingl, K. Yvon, L.G. Akselrud, A.V. Kolomietz, L. Havela, T. Vogt, I.R. Harris, B.C. Hauback, J. Alloys Comp. 279 (1998) 4.
[2] M. Yoshida, E. Akiba, Y. Shimojo, Y. Morii, F. Izumi, J. Alloys Comp. 231 (1995) 755.
[3] F. Gingl, K. Yvon, I.Yu. Zavaliy, V.A. Yartys, P. Fischer, J. Alloys Comp. 226 (1995) 1.
[4] H.N. Bordallo, H. Nakotte, J. Eckert, A.V. Kolomiets, L. Havela, A.V. Andreev, H. Drulis, W. Iwasieczko, J. Appl. Phys. 83 (1998) 6986.

[5] B.C. Hauback, H. Fjellvåg, L. Pålhaugen, V.A. Yartys, K. Yvon, in preparation.
[6] A.E. Dwight, M.H. Mueller, R.A. Conner Jr., J.W. Downey, H. Knott, Trans. Met. Soc. AIME 242 (1968) 2075.
[7] A.C. Larson, R.B. von Dreele, General Structure Analysis System (GSAS), LANSCE, MS-H 805 (1994).
[8] J. Rodriguez-Carvajal, FULLPROF: A program for Rietveld refinement and pattern matching analysis, Abstr. of the Satellite Meeting on Powder Diffraction of the XV Congress of the IUCr, 1990, p. 127.
[9] A. Kolomiets, L. Havela, V.A. Yartys, A.V. Andreev, J. Alloys Comp. 253/254 (1997) 343.
[10] G. Ehlers, H. Maletta, Z. Phys. B99 (1996) 145.